Journal of volcanology and geothermal research

Journal of Volcanology and Geothermal Research 98 (2000) 153–171

www.elsevier.nl/locate/jvolgeores

Voluminous lava-like precursor to a major ash-flow tuff: low-column pyroclastic eruption of the Pagosa Peak Dacite, San Juan volcanic field, Colorado

O. Bachmann[a,*], M.A. Dungan[a], P.W. Lipman[b]

[a]Section des Sciences de la Terre de l'Université de Genève, 13, Rue des Maraîchers, 1211 Geneva 4, Switzerland
[b]US Geological Survey, 345 Middlefield Rd, Menlo Park, CA, USA

Received 26 May 1999; received in revised form 8 November 1999; accepted 8 November 1999

Abstract

The Pagosa Peak Dacite is an unusual pyroclastic deposit that immediately predated eruption of the enormous Fish Canyon Tuff (~5000 km^3) from the La Garita caldera at 28 Ma. The Pagosa Peak Dacite is thick (to 1 km), voluminous (>200 km^3), and has a high aspect ratio (1:50) similar to those of silicic lava flows. It contains a high proportion (40–60%) of juvenile clasts (to 3–4 m) emplaced as viscous magma that was less vesiculated than typical pumice. Accidental lithic fragments are absent above the basal 5–10% of the unit. Thick densely welded proximal deposits flowed rheomorphically due to gravitational spreading, despite the very high viscosity of the crystal-rich magma, resulting in a macroscopic appearance similar to flow-layered silicic lava. Although it is a separate depositional unit, the Pagosa Peak Dacite is indistinguishable from the overlying Fish Canyon Tuff in bulk-rock chemistry, phenocryst compositions, and $^{40}Ar/^{39}Ar$ age.

The unusual characteristics of this deposit are interpreted as consequences of eruption by low-column pyroclastic fountaining and lateral transport as dense, poorly inflated pyroclastic flows. The inferred eruptive style may be in part related to synchronous disruption of the southern margin of the Fish Canyon magma chamber by block faulting. The Pagosa Peak eruptive sources are apparently buried in the southern La Garita caldera, where northerly extensions of observed syneruptive faults served as fissure vents. Cumulative vent cross-sections were large, leading to relatively low emission velocities for a given discharge rate. Many successive pyroclastic flows accumulated sufficiently rapidly to weld densely as a cooling unit up to 1000 m thick and to retain heat adequately to permit rheomorphic flow. Explosive potential of the magma may have been reduced by degassing during ascent through fissure conduits, leading to fracture-dominated magma fragmentation at low vesicularity. Subsequent collapse of the 75×35 km^2 La Garita caldera and eruption of the Fish Canyon Tuff were probably triggered by destabilization of the chamber roof as magma was withdrawn during the Pagosa Peak eruption.

Keywords: pyroclastic flow; rheomorphic flow; ash-flow tuff

1. Introduction

Most eruptions of silicic magma involve either relatively quiet effusions of lava or high-energy plinian columns in which fragmentation of magma is efficient and the associated pyroclastic deposits consist mainly of fine ash and highly vesiculated

* Corresponding author.
E-mail addresses: bachmann@sc2a.unige.ch (O. Bachmann), dungan@sc2a.unige.ch (M. Dungan), plipman@mojave.wr.usgs.gov (P. Lipman).

0377-0273/00/$ - see front matter
PII: S0377-0273(99)00185-7

Table 1
Summary of total-fusion ages on sanidine phenocrysts, Fish Canyon magmatic system. All ages calculated relative to 28.34 Ma Taylor Creek sanidine (Renne et al., 1998). Analyses done in the Geneva $^{40}Ar/^{39}Ar$ laboratory

Unit (in stratigraphic order)	Mean age (Ma)	Error (2σ)	Number of analysis
Nutras Creek Dacite	28.06	0.16	11
Fish Canyon Tuff	28.03	0.18	11
Pagosa Peak Dacite	27.93	0.18	11

pumice. Low-energy pyroclastic fountaining intermediate between these extremes has been inferred for a few eruptions that were characterized by unusual magmatic or eruptive conditions, such as low viscosity magmas (Mahood, 1984; Duffield, 1990; Turbeville, 1992) or syneruptive piecemeal collapse (Branney and Kokelaar, 1992). Where effusive and primary explosive activity occur during the same eruptive episode, effusion of lava commonly follows a more explosive initial phase (Eichelberger et al., 1986), although the reverse has been documented (Hildreth and Drake, 1992). Progressions from explosive to effusive activity are conventionally ascribed to vertical volatile gradients in stratified magma chambers, or alternatively to degassing of magma in a shallow magma reservoir or during ascent through permeable conduits (Fink et al., 1992).

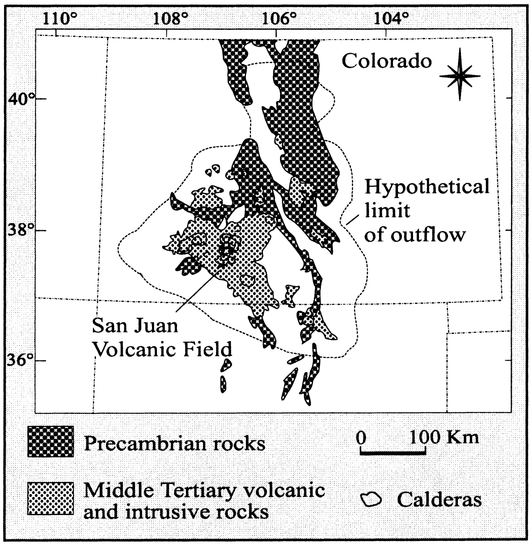

Fig. 1. Location of the San Juan volcanic field and related Tertiary extrusive and intrusive rocks in Colorado and New Mexico (Steven, 1975).

This paper describes initial eruptions of homogeneous crystal-rich dacite from an enormous magma reservoir, which we refer to as the Fish Canyon magmatic system. Three distinct phases of activity differing in eruptive mechanism, volume, and vent geometry were produced from the same magma chamber, apparently in rapid succession at ~28 Ma (Table 1). No important compositional distinctions (bulk composition, phenocryst modes, or mineral chemistry) have been detected among these three phases (Lipman et al., 1997). The second (main) eruptive phase is the Fish Canyon Tuff, a vast (~5000 km^3) ignimbrite erupted during the formation of the La Garita caldera. The last phase is a post-resurgence lava-like unit of small-volume (<1 km^3) within the caldera.

The Pagosa Peak Dacite, produced during the first phase of activity, is an unusual pyroclastic deposit. It has a volume of ~200 km^3, is locally >1 km thick, and is characterized by primary pyroclastic structures that differ vastly from the Fish Canyon Tuff. Although some basal flow units of the Pagosa Peak Dacite resemble typical pumiceous ignimbrite deposits, more than 90% of the deposit consists of a high proportion (40–60%) of poorly vesiculated magmatic fragments in a fine-grained matrix that lacks bubble-wall shards. The flow units are densely welded in all but a few basal and distal localities, and welding breaks are rare. Much of the densely welded material is massive or flow layered, resembling lava, and these features are interpreted as the consequences of rheomorphic flow. Severe fluidal deformation has rarely been documented for such a viscous pyroclastic deposit containing abundant phenocrysts in a silicic matrix; heat must have been efficiently retained during emplacement. Magma ascent along syneruptive faults, as opposed to catastrophic escape along a caldera margin, may have been a critical factor in producing the unusual characteristics of the Pagosa

Peak Dacite. Gas escape during ascent may have decreased the explosive potential of the magma, leading to low vesicularity and inefficient fracture-dominated fragmentation. The apparent absence of deposits analogous to the Pagosa Peak Dacite in the geological record may derive in part from the large volume of its magma reservoir, and perhaps from limited preservation of diagnostic features in units of similar origin but lower phenocryst content and magma viscosity.

2. Geological setting

2.1. San Juan volcanic field

The Oligocene San Juan volcanic field of southern Colorado (Fig. 1) is an erosional remnant of volcanism that covered much of the Southern Rocky Mountains during mid-Tertiary time (Larsen and Cross, 1956; Lipman et al., 1989). San Juan volcanic rocks now cover an area of about 25,000 km^2 and have a total volume close to 40,000 km^3. The eruptive products consist mainly of Oligocene calc-alkaline intermediate-composition lavas and silicic ash-flow tuffs, resulting from low-angle subduction under the North American plate (Lipman et al., 1978) or melting of lithospheric mantle previously modified by Proterozoic subduction (Davis et al., 1993). This sequence is locally overlain by thin Mio-Pliocene basaltic flows and minor rhyolite (mainly 26–20 Ma), related to the opening of the Rio Grande rift.

The Oligocene volcanism progressed from intermediate-composition calc-alkaline lavas and breccias to large silicic ash-flow sheets (Lipman et al., 1978). Eruptive activity began at approximately 35 Ma, as scattered stratovolcanoes produced large quantities of dominantly andesitic lavas and breccias. From 30 to 26 Ma, volcanism became more explosive, and at least 17 major silicic (~64–72% SiO_2) ash-flow sheets (100–5000 km^3) erupted from three caldera clusters. The western and southeastern (Platoro caldera complex) clusters were active concurrently from about 30 to 28 Ma. During the waning stages of ash-flow tuff volcanism in the Platoro complex (Lipman et al., 1996), caldera-related activity shifted to the center of the field at approximately 28.6 Ma, where it remained until dominantly calc-alkaline magmatism was succeeded by bimodal, dominantly basaltic rift-induced activity. The long-term evolution of the calc-alkaline volcanism is thought to record emplacement of a composite batholithic complex at shallow depth beneath the volcanic field, in accord with a large negative gravity anomaly centered on this region (Plouff and Pakiser, 1972; Lipman et al., 1978).

2.2. Fish Canyon magmatic system

The Fish Canyon Tuff, erupted from the La Garita caldera, is the second and largest of eight major ash-flow sheets erupted from the productive central San Juan caldera cluster, which generated approximately 8000 km^3 of silicic deposits through eight caldera-related eruptions during <2.5 million years (Lipman, 2000). Fish Canyon magma is compositionally unzoned crystal-rich dacite (35–45% crystals; 68.5% SiO_2) with a near-solidus mineral assemblage of two feldspars, hornblende, biotite, quartz, sphene, apatite, zircon and Fe–Ti oxides in silicic (~76% SiO_2) matrix glass (Whitney and Stormer, 1985). Preceding and subsequent caldera eruptions of the central San Juan cluster are characterized by diverse magmas, distinct in bulk composition and mineralogy from the Fish Canyon magma (Riciputi et al., 1995; Lipman, 2000). In contrast, the distinctive Fish Canyon magma type was erupted as the Pagosa Peak and Nutras Creek Dacites both before and after subsidence of the La Garita caldera.

Reinvestigation of the eruptive products of the Fish Canyon magmatic system, in connection with an overall reassessment of the central San Juan caldera cluster (Lipman, 2000), has revealed several previously unrecognized features. Estimates of the dimensions of the La Garita caldera and the volume of the Fish Canyon Tuff have been revised upward (Lipman et al., 1997), in light of the fact that the southern margin of the caldera is 30 km further south than previously recognized (Fig. 2). This complex collapse feature comprises three overlapping depressions that form a composite caldera elongated north–south, with aggregate dimensions of 75 × 35 km (area >2500 km^2). By assuming: (1) an average subsidence throughout the caldera of 1 km (variable but locally probably much greater); and (2) approximately co-equal proportions of intracaldera and outflow tuff

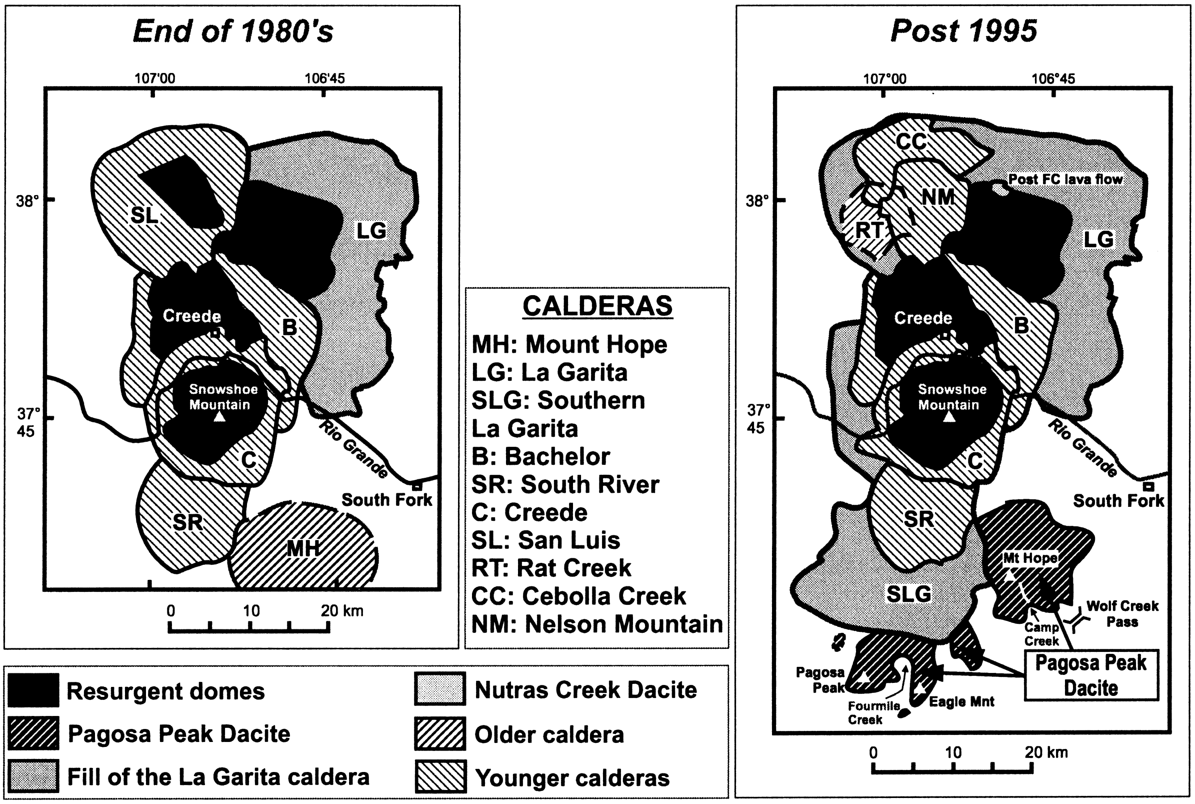

Fig. 2. Maps on the central caldera cluster of the San Juan volcanic field, as known at the end of the 1980s (Lipman et al., 1989) and after 1995 (Lipman, 2000).

a large but unknown volume of the outflow tuff has been eroded), we arrive at a crude but conservative estimate of 5000 km^3 for the volume of erupted Fish Canyon Tuff.

The nonresurgent southern depression is spatially associated with the precaldera Pagosa Peak Dacite, as well as voluminous intracaldera and extracaldera lavas and breccias of the postcollapse Huerto Andesite. By contrast, the northern segment, which is resurgent and lacks associated precursory eruptions of Fish Canyon magma or voluminous postcollapse andesitic volcanism, includes a post-resurgence lava flow of Fish Canyon type, the Nutras Creek Dacite (Fig. 2). The central depression is largely filled with and modified by younger nested calderas but may have been resurgent. No precursory activity has been identified in this sector that relates directly to the Fish Canyon magmatic system, but the northernmost vents for the postcollapse Huerto Formation are near its southwestern margin.

Although the mineralogy and mineral chemistry of the Pagosa Peak Dacite, Fish Canyon Tuff, and Nutras Creek Dacite are virtually identical, granophyric overgrowths form rims on shattered feldspars megacrysts in the last-erupted phases of the magmatic system (Lipman et al., 1997). These distinctive overgrowths occur only in intracaldera Fish Canyon Tuff of the northern depression and in Nutras Creek Dacite. This temporal and spatial zonation is ascribed to late syneruptive crystallization of granophyre during depressurization related to the precursory Pagosa Peak Dacite eruption and early collapse of the southern depression. On this basis, and the asymmetric distribution of the Pagosa Peak Dacite, eruption of the Fish Canyon Tuff is inferred to have progressed from south to north. This shift must have occurred rapidly, as the outflow Fish Canyon Tuff is a single compound cooling unit lacking granophyric overgrowths.

3. Pagosa Peak Dacite

The Pagosa Peak Dacite is preserved over an area of 350–400 km^2 around the southeastern margin of the La Garita caldera (Fig. 2). Distal nonwelded facies are rarely exposed, due to post-Oligocene erosion or burial by the Fish Canyon Tuff. Many features in the deposits suggest transport toward the south and southeast, and the initial depositional area may have exceeded 600 km^2. No eruptive sources for the Pagosa Peak Dacite are exposed; they are inferred to be buried within the southern La Garita caldera, along with as much as a third of the volume of the original deposit.

The Pagosa Peak Dacite is preserved primarily as two thick lobes (800 m to the south at Pagosa Peak, >1000 m to the east at Mount Hope), separated by an intervening thinner zone (<100 m) centered on Saddle Mountain. Thickness tends to decrease away from the caldera, and the preserved lateral extent does not exceed 15 km beyond the caldera wall. Termination of the deposits tends to be abrupt, in part due to selective erosion of the weakly welded distal facies. Although many sections are not exposed to their base, thickness is widely >300 m, and accumulations may have been even greater near the vents, implying a total volume in excess of 200 km^3. Thus, the aspect ratio (average thickness/horizontal extent; Walker, 1983) of the preserved remnants of the unit is ~1:50, more similar to large silicic lava flows than typical ignimbrites (~1:500 to 1:1000).

The Pagosa Peak Dacite was erupted prior to the Fish Canyon Tuff, but from the same magma chamber. Evidence for this relation includes: (1) indistinguishable mineralogy, mineral chemistry, and magma compositions of the two units; (2) truncation of the Pagosa Peak Dacite by the southern margin of the La Garita caldera; and (3) deposition of Fish Canyon Tuff directly on the Pagosa Peak. The time interval between these two units is inferred to have been brief. Where the contact is exposed, neither a soil horizon nor an erosional surface is present, suggesting emplacement in rapid succession. $^{40}Ar/^{39}Ar$ ages of the three eruptive phases of the Fish Canyon magmatic system are indistinguishable (Table 1).

3.1. Macroscopic textures and structures

The Pagosa Peak Dacite differs from other eruptive phases of the Fish Canyon magmatic system, and from other eruptive products of the San Juan volcanic field, by the presence of unusual juvenile pyroclasts. These magmatic fragments are dense, subrounded to elliptical in shape, and are inferred to have been viscous at the time of emplacement (Fig. 3). They constitute high proportions of the rock relative to matrix (~50%). The typical size range for the Pagosa Peak pyroclasts is 20–60 cm; many exceed 1 m, and some are 3–4 m in diameter. We refer informally to these pyroclasts as magma blobs, to distinguish them from the rigid juvenile blocks characteristic of block-and-ash flows. The blobs are morphologically different from pumices in most silicic pyroclastic rocks, although similar lenticular fragments have been described in the Taylor Creek Rhyolite (Duffield, 1990). They have no relation to mafic enclaves resulting from magma mixing, for which the term "blob" is also sometimes applied; the Pagosa Peak blobs are fragments of dacitic Fish Canyon magma that are chemically indistinguishable from the matrix.

Flattening ratios of densely welded Pagosa Peak blobs <1:5 are rare, except where they are modified by rheomorphic flow. Even densely welded blobs commonly are subequant, although many are weakly elongate. Neither composite blobs nor evidence for incorporation of previously fragmented and welded material has been recognized. Blob morphologies are subrounded to angular, contacts with the matrix are everywhere sharp, and fiamme-like interdigitations with matrix are absent. The subequant shapes of many blobs suggest limited compaction during welding, denoting relatively low vesicularity at the time of emplacement. The matrix (plus small blobs) does not compact differentially around larger blobs (Fig. 3b), even in densely welded units, indicating that primary porosity was comparable in both matrix and blobs.

Many blobs have internal mineral lineations or flow layering (Fig. 4), both in densely welded and nonwelded facies. Such fabrics within blobs are randomly oriented relative to depositional bedding, and some internal flow layering or mineral lineations are at high angles to the elongation of the blob. These relations indicate that the internal fabrics formed prior to fragmentation.

Two subunits of the Pagosa Peak Dacite are distinguished on the basis of accidental lithic fragments

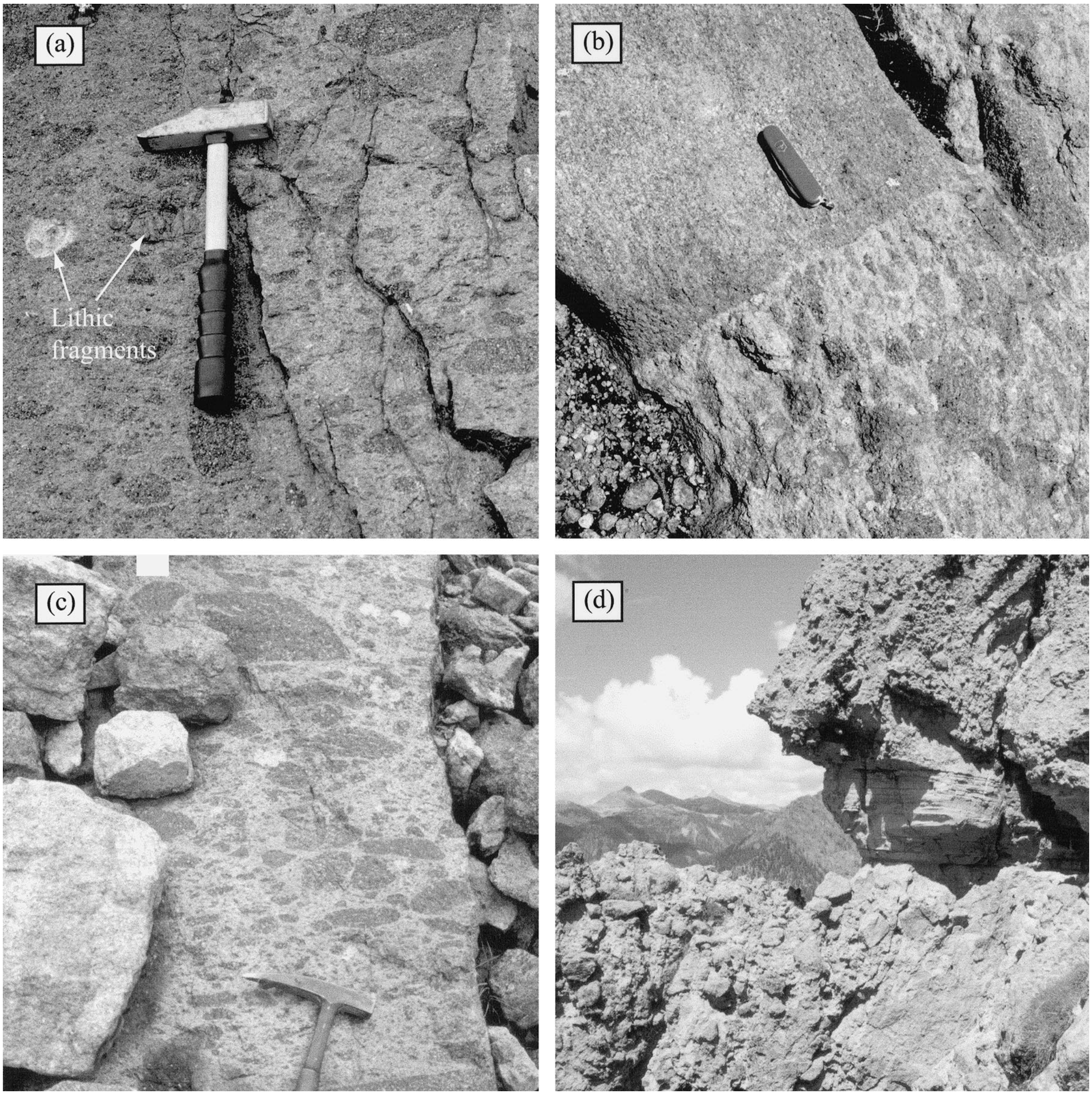

Fig. 3. Blob textures in the Pagosa Peak Dacite: (a) densely welded lithic-bearing deposit: glassy blobs have lenticular shapes and limited flattening foliation (south part of the east lobe); (b) penetrative deformation in a densely welded outcrop: small lenticular blobs trend directly into a larger angular block, indicating absence of differential compaction between block and matrix (NE of Wolf Creek Pass)—Knife is approximately 10 cm long; (c) lithic-free vitrophyre: textures are similar to those in lithic-bearing deposits of Fig. 3a (densely welded, limited compaction, glassy), although the blobs are larger, to 1.5 m (east lobe, at Camp Creek); (d) nonwelded flow units in distal lithic-free deposits, containing high proportion of blobs: surge-like interbeds at flow-unit break are 1.5 m thick (W side of Saddle Mountain).

(Fig. 5). Lithic-bearing deposits are confined to basal units and form less than 5–10% of the total volume. Most are blob-bearing pyroclastic-flow deposits, but minor pumiceous pyroclastic-flow, fallout, and surge deposits are also present. The distribution of lithic-bearing flow and surge deposits was controlled by pre-existing low-relief topography, and thickness ranges from a few meters to ~80 m. Accidental lithic fragments rarely exceed more than a few volume percent. Most are small andesitic fragments (to

Fig. 4. Flow-layered blob in distal, nonwelded Pagosa Peak Dacite, probably reflecting shearing during magma ascent. (E side of Saddle Mountain).

15–20 cm; Fig. 3a) that were probably incorporated in the flows during conduit erosion in the initial stage of activity.

The overlying lithic-free deposits are thick accumulations (averaging 300 m) of pyroclastic-flow deposits containing high proportions of blobs (Fig. 3c). Thickness of individual pyroclastic-flow units commonly is a few meters to >30 m. Such flow units apparently do not become finer-grained distally and are poorly sorted internally, although faint inverse grading can be present. Subhorizontal bedding is locally defined by the presence of multiple pyroclastic flows, especially in weakly welded distal sections, where surge-like interbeds separate flow units (Fig. 3d). Most proximal sections are massive, and flow-unit boundaries are obscure. Except for distal sections on Saddle Mountain, the lithic-free deposits are densely welded without breaks, even where >500–1000 m thick; rapid accumulation of many successive flow units is implied.

The base of the Pagosa Peak Dacite is everywhere vitrophyric, and glassy material is locally >200 m thick. In contrast, basal vitrophyres are rare in the Fish Canyon Tuff, and generally <5 m where present.

3.2. Microscopic textures

Fish Canyon magma contained about 40% phenocrysts, with diameters to 5 mm (~1–2 mm average), in a matrix of silicic rhyolite glass. In glassy samples the matrix is free of feldspar microlites. Most glasses contain minute filamental oxide grains resulting from incipient devitrification, not magmatic crystallization. Devitrified samples contain spherulites and crystallites similar to welded and devitrified ignimbrites.

Phenocrysts of feldspar (especially sanidine) and quartz are intricately corroded, and they contain numerous melt pockets (Fig. 6a). In large sanidine grains these pockets commonly contain inclusions of

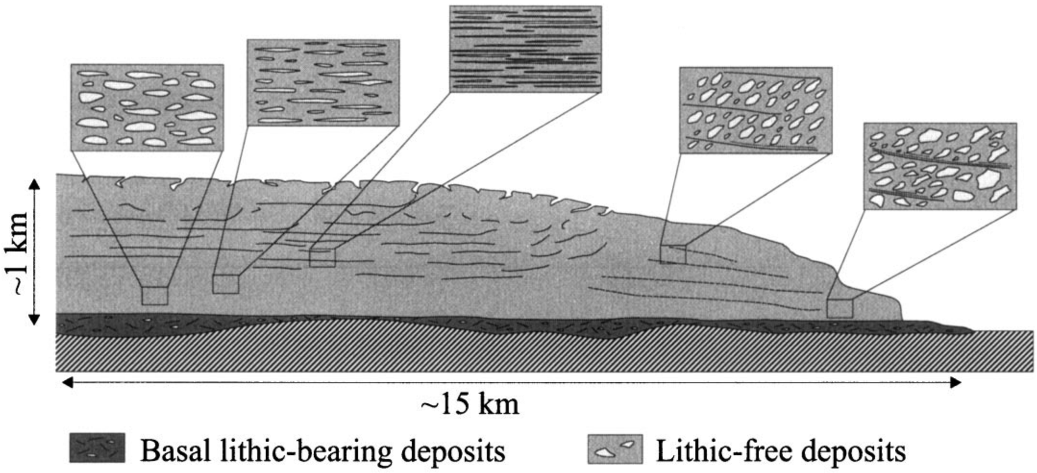

Fig. 5. Schematic stratigraphy of the Pagosa Peak Dacite, showing rough proportions between basal lithic-bearing and overlying lithic-free deposits. Inset boxes diagrammatically show progressive flattening of the blobs in proximal, upper part of the lithic-free deposits.

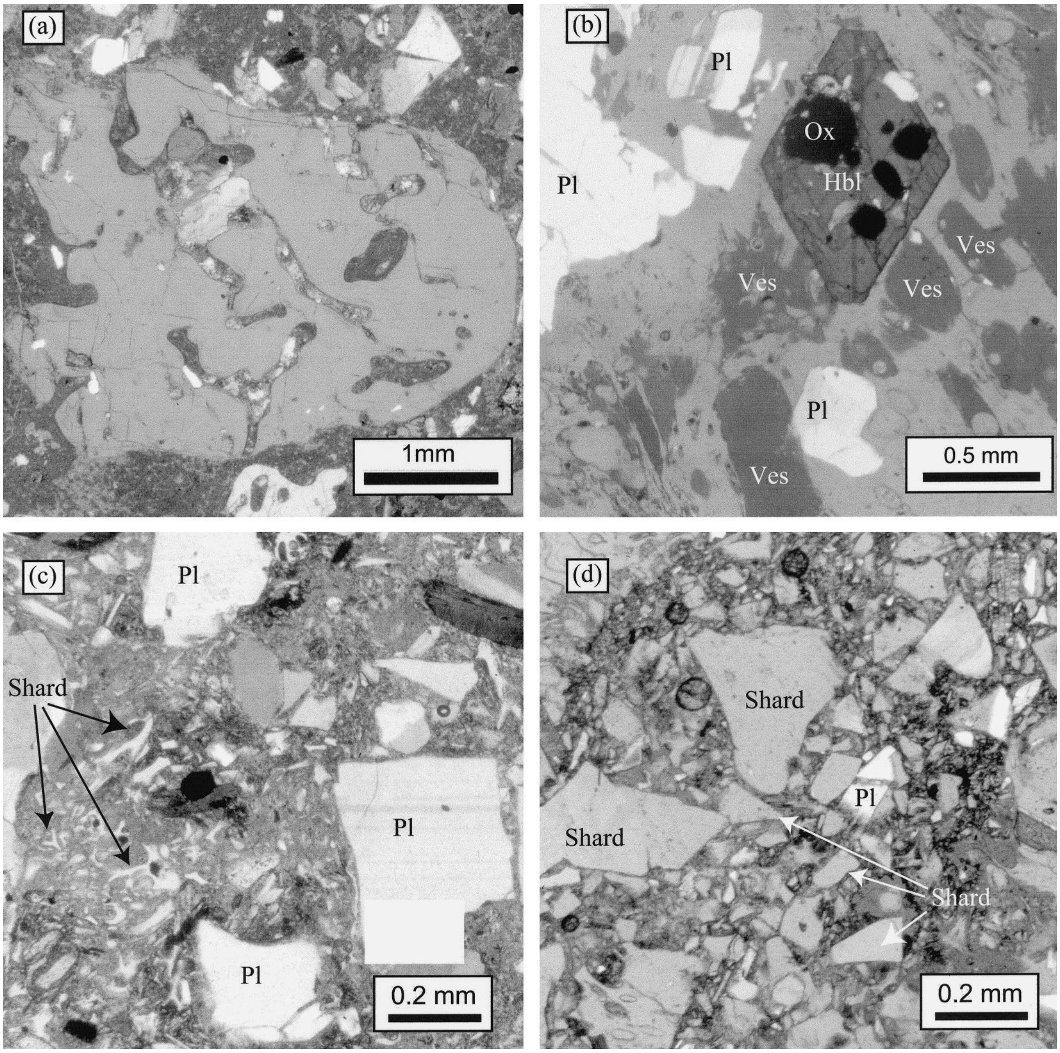

Fig. 6. Microscopic textures in rocks of the Fish Canyon magmatic system: (a) large (~5 mm) resorbed sanidine containing melt pockets and channels, in Pagosa Peak Dacite; (b) heterogeneously distributed vesicles in a nonwelded blob: most are elongated and show coalescence to form small clusters—vesicularity is ~25%; (c) matrix texture in nonwelded Fish Canyon Tuff: glass shards have the typical cuspate morphology of bubble walls; (d) matrix texture in a nonwelded blob—glass shards in the matrix are blocky, differing from the cuspate shapes of bubble-wall shards.

plagioclase, or more rarely of other phases. We interpret these resorption textures as consequences of the magma-generation process, not as melting related to eruption. Although these melt-laden crystals are potentially fragile during explosive volcanism due to internal expansion of exsolved vapor (Best and Christiansen, 1997), few crystals in the Pagosa Peak blobs are extensively broken. Many large feldspars in pumices of the northern intracaldera Fish Canyon Tuff are shattered and rimmed by granophyric overgrowths (Lipman et al., 1997), whereas "phenocrysts" in typical outflow Fish Canyon Tuff matrix are predominantly smaller, angular, fragments of broken crystals without granophyric overgrowths. Neither biotite nor hornblende exhibit the marginal breakdown textures documented in many calc-alkaline magmas (e.g. Devine et al., 1998; Rutherford and Hill, 1993). Both are typically euhedral and lack

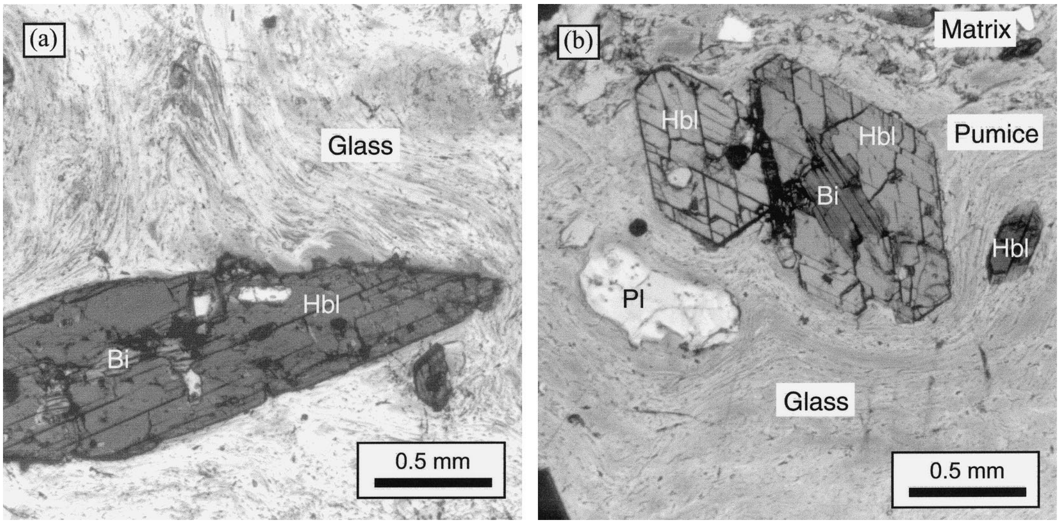

Fig. 7. Matrix flowage textures: (a) fluidal texture, surrounding euhedral hornblende in glassy matrix of Pagosa Peak Dacite, is enhanced by preferred orientation of small oxide filaments; (b) texture of welded pumice lens (bottom) in intracaldera Fish Canyon Tuff, containing euhedral hornblendes and a small corroded plagioclase. Flowage fabric is similar to that in Pagosa Peak blobs, due to annealing of vesicles upon welding.

evidence for the mineral-melt disequilibrium typical of quartz and sanidine (Fig. 7a and b).

Most blobs are dense and lack porosity as a consequence of welding. Glassy samples preserve fluidal textures, highlighted by minute oxide filaments that are locally aligned and wrap around phenocrysts (Fig. 7a), similar fiamme in the intracaldera Fish Canyon Tuff (Fig. 7b), and the Badlands lava flow (Manley, 1996). This similarity probably reflects the former presence of vesicles in blobs that were subsequently annealed during welding.

Table 2
Vesicularities of silicic pumices in comparison to the Pagosa Peak Dacite and Fish Canyon Tuff. The Fish Canyon value is approximate, due to lack of fresh, nonwelded pumices

Unit	Mean bulk vesicularity (%)	Bulk vesicularity (range in %)
Pagosa Peak Dacite	~ 25	18–35[a]
Fish Canyon Tuff	> 60	–
Bishop Tuff (Houghton and Wilson, 1989)	71	64–78
Taupo ignimbrite (Houghton and Wilson, 1989)	73	70–77
Average silicic pumices (Cashman and Mangan, 1994)	~ 75	70–80

[a] This range of bulk vesicularity translates into 30–50% matrix vesicularity if the magma averaged 40% phenocrysts.

In rare nonwelded to weakly welded flow units, elliptical to highly irregular vesicles are preserved in blobs (Fig. 6b). They are mostly <10–30 μm, although the size distribution is irregular and some are large (~500 μm). Due in part to high crystal contents, the vesicles are heterogeneously distributed as local clusters separated by dense zones. All vesicles are somewhat deformed, as indicated by elliptical to highly elongated shapes, suggesting vesicle collapse or a small component of shear.

Bulk-rock and glass vesicle contents were measured in thin sections impregnated with colored epoxy (Cashman and Mangan, 1994), assuming that vesicle orientation is quasi-random in two dimensions at thin section scale. Although limited in scope by the rarity of nonwelded samples and the heterogeneous distribution of vesicles, measured vesicularity is lower in the Pagosa Peak Dacite (Table 2) than in most pyroclastic deposits (Houghton and Wilson, 1989). Such low vesicularity is in accord with the limited flattening upon welding and lack of macroscopic interdigitations with matrix at the terminations of blobs. Reliable estimates of vesicularity in the Fish Canyon Tuff are more difficult to obtain, due to the small size of pumices, widespread dense welding, and spherulite growth in the glass.

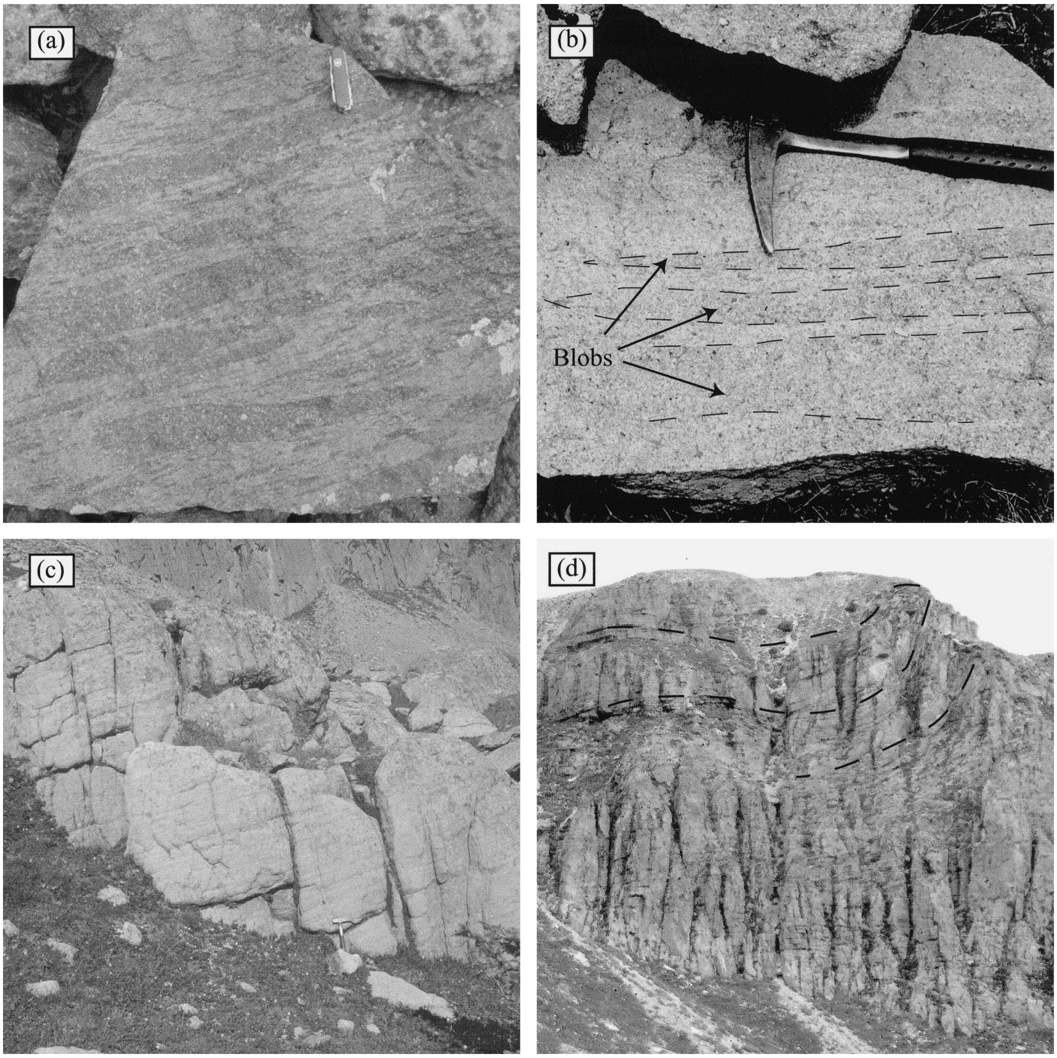

Fig. 8. Progressive upward flattening of primary pyroclastic fragments (blobs) until the rock resembles lava. (a) Elongated lenticular blobs in basal vitrophyre (west part of south lobe). (b) Devitrified interior of deposit, having elongated blobs with aspect ratios to 1:15 (Camp Creek); blob boundaries enhanced by dashed lines. (c) Foliated texture in devitrified rock, resembling flow-layered silicic lavas due to the elongation of blobs (Camp Creek). (d) Ramp structure, indicating flowage in upper parts the deposit (head of Camp Creek); foliation trends enhanced by dashed lines.

The fine-grained matrix of nondevitrified Pagosa Peak Dacite consists mostly of smaller, broken phenocrysts, glass shards, and fine crystal and glass dust. Preserved glass shards in these deposits are angular and equant (Fig. 6d) in contrast to the cuspate shapes of bubble-wall shards in the Fish Canyon Tuff (Fig. 6c) and other ignimbrites. Because vesicularity may be underestimated due to incipient collapse of vesicles following emplacement, the unusual shapes of glass shards in the Pagosa Peak Dacite are important evidence that vesicularity was comparatively low at the time of fragmentation. An origin for the ashy matrix of the Pagosa Peak Dacite by comminution during eruption and emplacement, rather than bubble-wall rupture due to high vesicularity, is consistent with the large dimensions of blobs, the lack of differential compaction during welding, and the heterogeneous distributions of irregularly shaped vesicles in Pagosa Peak blobs.

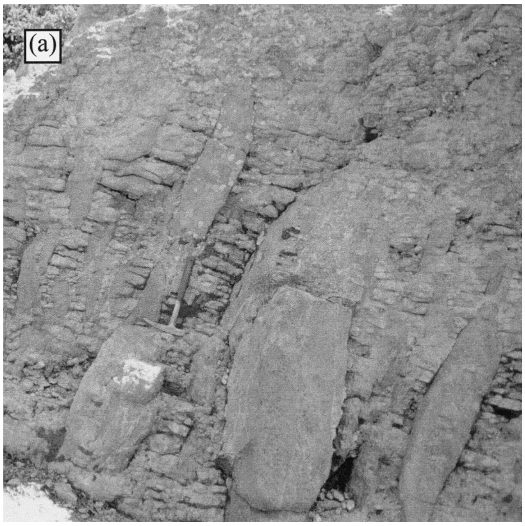

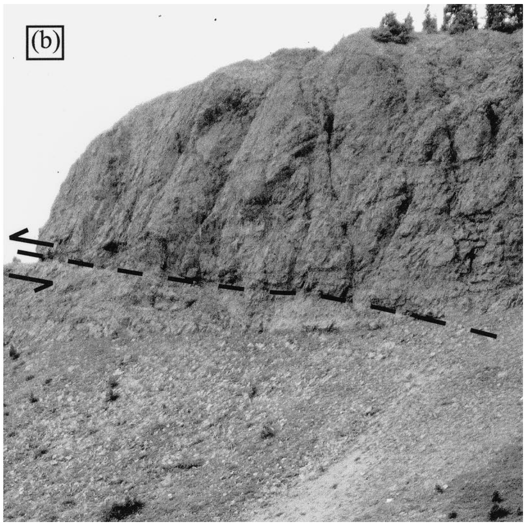

Fig. 9. Textures related to secondary brittle deformation. (a) Steeply dipping elongated blobs (to 1.5 m in long axis) south of Mount Hope; brittle pull-apart fractures cut matrix but not the blobs. (b) Subhorizontal thrust fault in a cliff face west of Wolf Creek Pass.

3.3. Rheomorphic flow

Pyroclastic textures, everywhere well preserved in the distal and lower parts of the lithic-free deposits, are partly to completely obliterated in the upper parts of thick proximal sections by extreme welding, rheomorphic flow, and devitrification. At a few tens to 150 m above the base, distinctions between increasingly flattened blobs and matrix become gradually obscure, and outcrop surfaces resemble weakly foliated lava (Fig. 8a–c). The foliation is defined by differences in crystal size between layers of similar thickness (a few cm), reflecting the larger size of nonbroken phenocrysts in flattened blobs relative to matrix.

The blobs are elongate parallel to the transport direction and flattened in the plane of the foliation, which is generally subparallel to the regional dip ($\sim$5–10° to NE). Gentle undulations in orientation are common, and foliations locally dip steeply in upper parts of several thick sections. Small-scale tight folds are rare, but the role of plastic flow is confirmed by ramp structures at two localities in the eastern lobe that resemble those in upper parts of large silicic lava flows (Fig. 8d). Orientations of the ramps are consistent with directions of flow away from the inferred vent region.

At the tops of some thick sections, the Pagosa Peak Dacite is brecciated where depositionally overlain by Fish Canyon Tuff. Such breccias are several meters thick, massive, and dense; they are characterized by coarse ($<$1 m) angular dacite blocks in a reddish oxidized matrix. Interpreted as carapace breccias, these provide further support for the inferred post-depositional flow.

Distal blob deposits near Wolf Creek Pass were deformed differently from the more widespread features just described. Large stretched and slightly flattened blobs (elongation ratios to 20:1, surfboard shapes in 3D) are spectacularly inclined to the northwest; dips, increase upward, to 70° at high stratigraphic levels (Fig. 9a). The matrix was more brittle, at least during late stages of deformation, as it contains well-developed pull-apart fractures. The only well exposed contact between blobs and overlying foliated rock in this area (a few km NE of Wolf Creek Pass) is abrupt. Within $<$2 m, well-developed blob-bearing material changes abruptly into weakly foliated massive rock, a discontinuity which suggests subhorizontal shear motion. The highest recognizable blobs are cut by vertical pull-apart fractures, and the presence of low-angle thrust faults (NE → SE) lower in this area (Fig. 9b) also attests to a component of late brittle deformation.

Rheomorphic flow has been recognized elsewhere in a few calc-alkaline tuffs (Chapin and Lowell, 1979;

Table 3
Compositions of two representative magmatic fragments in the Pagosa Peak Dacite (XRF) and interstitial glass (electron microprobe)

	Bfc83	Bfc91	Glass (Bfc83)
SiO_2	68.26	67.94	76.05
Al_2O_3	15.38	15.29	12.37
FeOt	3.55	3.79	0.26
MgO	0.92	1.09	0.05
CaO	2.91	2.95	0.60
Na_2O	3.92	3.94	2.66
K_2O	4.35	4.16	5.42
TiO_2	0.44	0.46	0.13
MnO	0.09	0.10	0.04
P_2O_5	0.18	0.19	0.02
Total	99.99	99.91	97.77

Smith and Cole, 1997), but is more common in low-viscosity peralkaline deposits (Schmincke and Swanson, 1967; Mahood, 1984; Mahood and Hildreth, 1986) and high-temperature crystal-poor units (Milner et al., 1992; Twist and Elston, 1989). The Pagosa Peak Dacite, with its near-solidus mineral assemblage in a rhyolitic matrix and relatively low magmatic temperature, was more viscous than most pyroclastic rocks that display fluidal deformation. Rapid deposition and exceptionally efficient heat retention seem required.

3.4. Magma water content and viscosity

Fish Canyon magma was homogeneous, crystal-rich dacite (Table 3), reflecting near-solidus conditions, in agreement with the inferred magmatic temperature of 760 ± 30°C (Johnson and Rutherford, 1989). This temperature and the presence of biotite and hornblende at 2.5 kbar suggest a high water content, estimated at 5 wt% (Johnson and Rutherford, 1989).

Calculated magma viscosities of extrusive silicic magma are 10^4–10^6 Pa s (Scaillet et al., 1998). Fish Canyon magma viscosity is near the upper end of this range, both matrix melt viscosity ($\sim 10^{5.2}$ Pa s) calculated by the method of Hess and Dingwell (1996) at 5 wt% H_2O, and bulk viscosity ($\sim 10^6$ Pa s) calculated using their Eq. (2).

4. Syneruptive subsidence structures

Subsidence during eruption of the Pagosa Peak Dacite is characterized by block faulting that produced a broad zone of grabens and horsts, similar to that described as piecemeal subsidence (Branney and Kokelaar, 1994; Moore and Kokelaar, 1998), rather than collapse of a piston-like caldera. The faulted area is within the southern lobe of the Pagosa Peak Dacite, immediately south of the La Garita caldera (Fig. 10). Subvertical normal faults trending NE and NW, some with displacements >500 m, form two grabens 3–4 km wide. They are separated by a horst to the south but merge northward near the southern topographic wall of the caldera. The La Garita wall truncates these faults, indicating that they extended into the region that collapsed during eruption of the Fish Canyon Tuff.

No significant fault movement has been recognized prior to eruption of the Pagosa Peak Dacite, but major faulting was concurrent with its eruption. Landslide blocks derived from underlying footwall units are locally intercalated with Pagosa Peak pyroclastic flows adjacent to fault scarps, and drastic changes in thickness of the Pagosa Peak Dacite across such faults indicate that large displacements were contemporaneous with its emplacement. Deformation of Pagosa Peak Dacite adjacent to a fault scarp at Eagle Mountain was apparently related to fault movement prior to complete solidification (Fig. 11).

Faulting outside the caldera ceased at the onset of caldera collapse; Fish Canyon Tuff overlaps these faults without offset. In contrast, extensional faulting continued inside the caldera during and slightly after the emplacement of the postcaldera Huerto Andesite (Fig. 10). Several northwest-trending faults with vertical displacements of 50–250 m cut the Huerto Andesite but are covered without offset by the younger Carpenter Ridge Tuff.

The southern La Garita wall is locally faulted, and two linear segments of the caldera margin that are subparallel to trends of Pagosa Peak-related faults intersect at an acute angle northwest of Saddle Mountain (Fig. 10). These faults appear to have formed in part during the collapse of the caldera, and in part during a younger Huerto-related episode. The subparallelism of La Garita caldera margins to syn-Pagosa Peak faults trends suggests that these

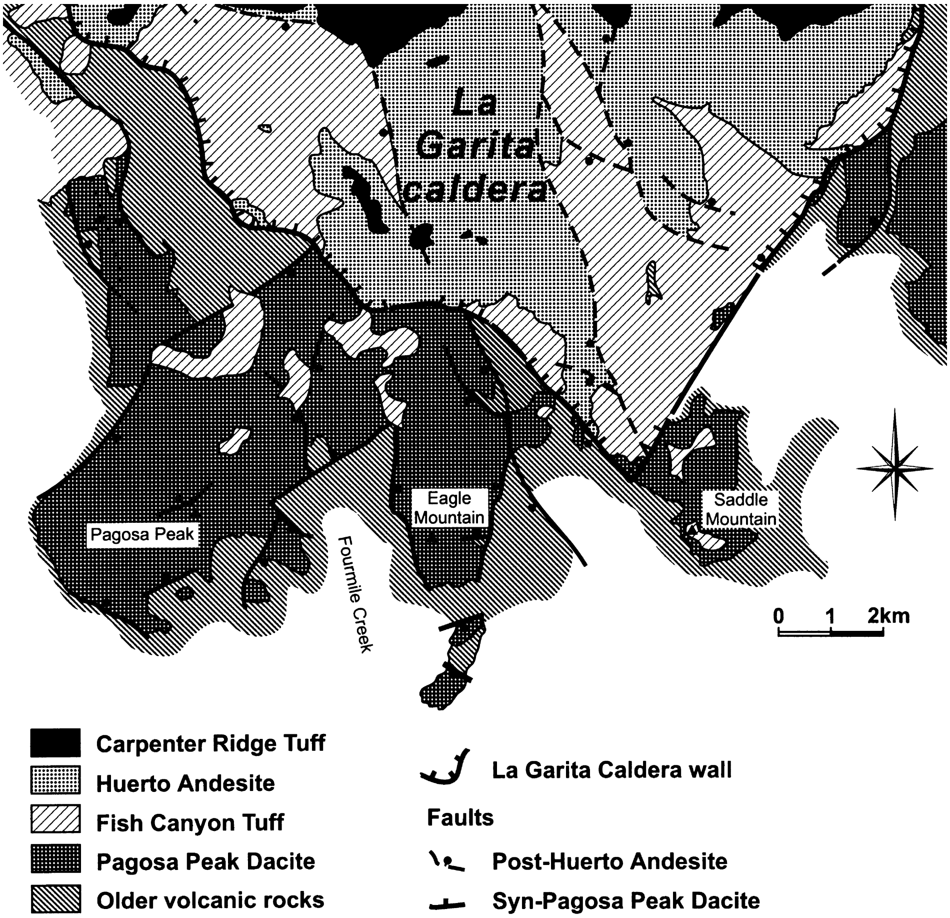

Fig. 10. Map of the southern part of the La Garita caldera, showing faults active during eruption of the Pagosa Peak Dacite. These faults form a complex graben aligned with the N–S axis of the La Garita caldera, having two deep segments separated by a horst. Units predating the Pagosa Peak Dacite include older tuffs (Masonic Park and Chiquito Peak Tuffs) and andesites (Conejos Formation and Sheep Mountain Andesite).

pre-existing faults played a role in localizing the southern caldera structures.

Vents for the Pagosa Peak Dacite are probably buried within the southern segment of the La Garita caldera. Syneruptive extensional faults that project into the caldera area may have served as magma conduits, as indicated by general parallelism with post-Huerto faults within the caldera that suggest sustained influence by early structures.

5. Eruptive mechanisms

Many observations indicate that pyroclastic flows were the primary emplacement mechanism for the Pagosa Peak Dacite, but this exceptionally thick composite unit differs from typical ignimbrites, including the Fish Canyon Tuff. It is characterized by high aspect ratios, a near absence of accidental lithic fragments, and a high proportion of large subequant blobs that are distinct in size, shape, and vesicle content from typical pumices. These features resemble those of block-and-ash flows related to dome collapse (e.g. Rodriguez-Elizarras et al., 1991; Ui et al., 1999), but such an emplacement mechanism seems improbable for the Pagosa Peak Dacite.

Fig. 11. Steep flow layering in brecciated Pagosa Peak Dacite, adjacent to fault at Eagle Mountain.

5.1. Dome collapse or low-column fountaining of silicic magma?

Formation of the Pagosa Peak Dacite by dome collapse would require the extrusion of an immense lava-dome complex that shed block-and-ash flows in rapid succession as the flanks of active domes became gravitationally unstable. The Pagosa Peak deposits are extraordinarily voluminous and thick in comparison to well-documented dome-related block-and-ash flows. These are typically small volume ($<0.01\ km^3$), represent only a fraction of the parental-dome volume, and have runout distances of only a few kilometers (Cole et al., 1998). The near-vent topographic relief needed to deposit the Pagosa Peak as an accumulation of gravitationally-emplaced block-and-ash flows more than 1 km thick would require the growth of domes to extraordinary heights. Such a dome complex would have been entirely inboard of the topographic rim of the La Garita caldera, as no remnants are preserved.

Additional features of the Pagosa Peak Dacite require rapid emplacement and efficient heat retention during deposition. It is uniformly glassy near the base, becomes thoroughly devitrified upward, largely lacks welding breaks, and was deformed by post-emplacement flow. Clasts in block-and-ash flows are typically variably devitrified, in contrast to the absence of devitrified clasts in the glassy basal Pagosa Peak Dacite. Block-and-ash flow deposits are also nonwelded or at most weakly cintered (Boudon et al., 1993), in contrast to the unified welding-crystallization zonation that encompasses multiple flow units in the Pagosa Peak Dacite. The extrusion of lava, followed by gravitational collapse on the flanks of immense domes, is an inefficient heat-retentive mechanism, not compatible with the high emplacement rate indicated by the simple welding zonation of the Pagosa Peak Dacite. Intense post-emplacement viscous flow is also more difficult to reconcile with initial emplacement as block-and-ash flows than with magma fragmentation in the eruptive conduit and primary pyroclastic eruption.

A sustained low-column eruption from fissures, and lateral transport in poorly inflated, low-momentum pyroclastic flows, is our favored model for the rapid emplacement and efficient heat retention that these deposits appear to require. Many characteristics of the deposits (high aspect ratio, near absence of lithic fragments, high proportion of poorly vesiculated blobs, absence of shattered crystals) suggest lower emission velocities than typical ignimbritic eruptions (Wilson et al., 1980; Wilson et al., 1995; Best and Christiansen, 1997). A fracture-dominated magma fragmentation mechanism is apparently required by the large sizes and the angular shapes of magmatic blobs, as well as by the near absence of typical bubble-wall shards in the ashy matrix of these deposits. These unusual characteristics may reflect high viscosity at fragmentation, induced by gas escape during magma ascent, and high strain rate in the conduits as recorded by the flow layering in many blobs (Fig. 4).

Measured vesicularity in pyroclasts of high-viscosity magmas, such as the Fish Canyon, are effective recorders of vesicularity at fragmentation (Gardner et al., 1996; Klug and Cashman, 1996). The bulk vesicularity of Pagosa Peak magmatic blobs is lower than that in typical silicic pumices (Cashman and Mangan, 1994). Even the vesicle content in matrix glass is much lower than the 60–70% threshold (Table 2) that is commonly cited for in-conduit fragmentation induced by bubble-wall rupture (Sparks, 1978; Gardner et al., 1996). The limited welding-related flattening of blobs in glassy Pagosa Peak Dacite is consistent with the low vesicle contents of nonwelded samples, implying fragmentation at vesicularity levels well below the typical threshold. A phreatomagmatic component to the eruption might contribute to fragmentation at low vesicularity (Houghton and Wilson, 1989), but the coarse clast size, large total volume, and absence of accidental lithic fragments in most of the deposit are inconsistent with such a mechanism.

5.2. Syneruptive degassing?

The eruption of the Pagosa Peak Dacite, the Fish Canyon Tuff, and the postcaldera lava-like Nutras Creek Dacite from the same homogeneous magma chamber suggests that differences in eruptive style were independent of pre-eruptive magma characteristics, and that these differences arose from syneruptive processes in magmatic conduits. The diversity of such processes is also emphasized by apparently quiescent eruption of the Chao dacite (Chile; de Silva et al., 1994), the largest known Quaternary eruption of silicic lava (24 km^3), which is compositionally similar to units of the Fish Canyon magmatic system. Factors influencing the unusual eruptive and deposition features of the Pagosa Peak Dacite seem to include a delicate balance between gas loss in the conduit and rate of magma ascent.

Gas loss through conduit walls from magma ascending as a permeable foam has been widely recognized as an important control on eruptive styles of silicic magmas (Eichelberger et al., 1986; Jaupart and Allègre, 1991; Woods and Koyaguchi, 1994; Stasiuk et al., 1996). Protracted syneruptive degassing and attendant viscosity increase (Dingwell et al., 1996; Sparks, 1997) during rise of the Pagosa Peak magma may have contributed to its low vesicularity at fragmentation and the difference between this eruption and the Fish Canyon Tuff. Magma fragmentation during sustained silicic eruptions is thought to occur when the strain rate overcomes magma relaxation time, a parameter inversely proportional to viscosity (Dingwell and Webb, 1989). This process implies a correlation between void fraction and viscosity at fragmentation, observed both in natural pumices (Thomas et al., 1994) and by numerical simulations (Papale, 1999). Efficient degassing coupled with high shear stress during ascent, as suggested by the ubiquitous inherited flow layering in blobs, could thus have provoked brittle fracturing of the magma at a low vesicularity and the low inferred explosivity of the Pagosa Peak eruption may be a direct consequence of inefficient fragmentation, as the amount of exsolved gas available to expand explosively at fragmentation was limited.

Two indicators of extensive degassing of initially water-rich magmas are reaction rims on amphibole phenocrysts (Rutherford and Hill, 1993) and nucleation of plagioclase microlites in matrix liquid due to elevation of the solidus temperature (Geschwind and Rutherford, 1995; Hort, 1998). The absence of such textures in all eruptive phases of the Fish Canyon magmatic system suggests that degassing during the Pagosa Peak eruption occurred under a restricted range of conditions. Required are ascent rates that permitted vesiculation, efficient degassing, fragmentation, and eruption without amphibole breakdown or microlite nucleation.

Studies of recent eruptions of magmas close in bulk composition and mineralogy to the Fish Canyon magma, in part calibrated by experimental studies, provide limits on the rates of these two processes. Hornblende breakdown occurs within days or hours of magma ascent. Dacite erupted at Mount St. Helens (~930°C) is less evolved than the Fish Canyon magma, but crystal-rich andesite forming the active dome on the Island of Montserrat (~830°C) is characterized by interstitial liquid compositions like the Fish Canyon magma. For both eruptions, hornblende phenocrysts have well-developed reaction rims and the matrix contains microlites, interpreted as resulting from pre-eruptive vapor loss (Rutherford and Hill, 1993; Sparks, 1997; Devine et al., 1998). The rhyolitic Inyo Domes, for which the permeable-foam hypothesis was first proposed (Eichelberger et al., 1986), and the Chao Dacite both contain well-developed matrix microlites (Swanson et al., 1989; de Silva et al., 1994). Presence of microlites in rhyolite matrix (76% SiO_2) of Pinatubo dacite, erupted after repose periods >40 min, also suggests rapid degassing-induced nucleation (Hammer et al., 1999). The Pinatubo dacite, which is similar to the Fish Canyon magma in temperature and glass composition, lacks hornblende breakdown textures; microlite nucleation may be the more sensitive indicator of degassing.

These examples provide useful analogues for the Fish Canyon magma, although eruption temperatures

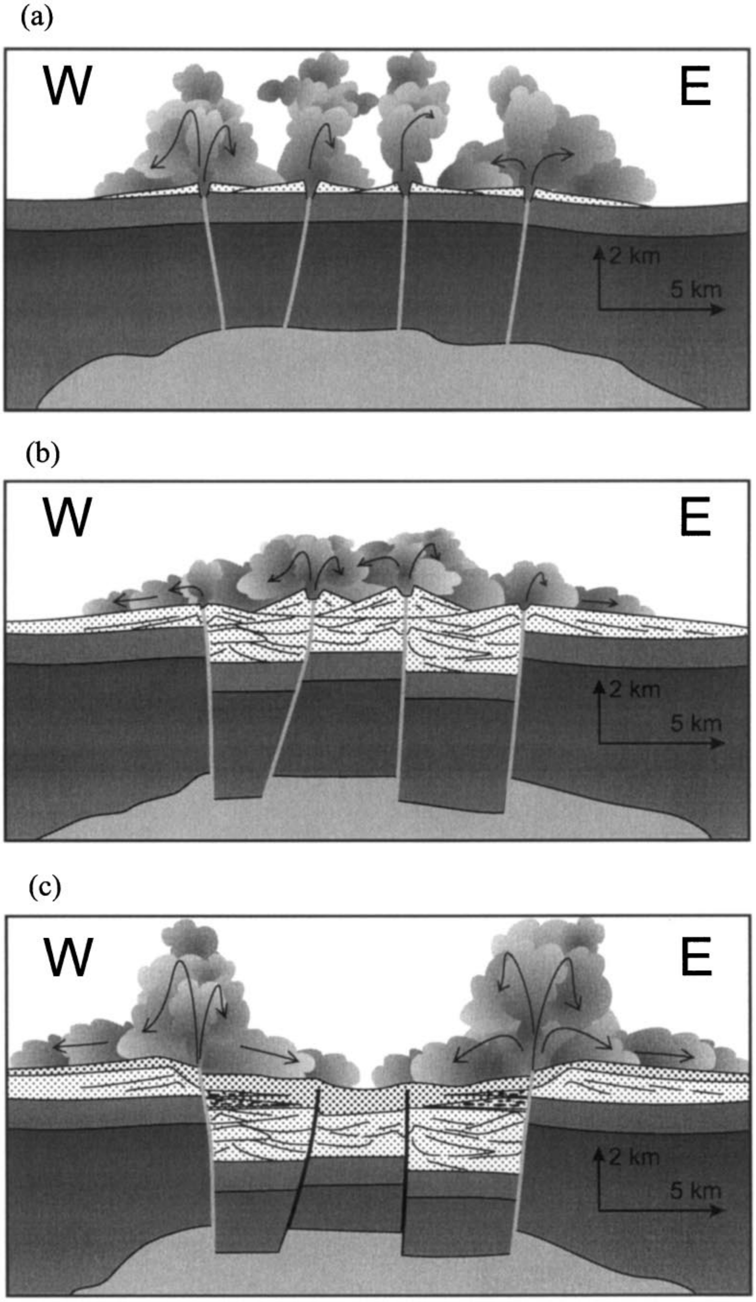

Fig. 12. Schematic processes during eruption of the Pagosa Peak Dacite and Fish Canyon Tuff: (a) early eruption of Pagosa Peak Dacite—emplacement of lithic-bearing deposits from multiple vents; (b) main stage of this eruption—low-column pyroclastic fountaining from fissure vents along syneruptive faults; (c) eruption of the Fish Canyon Tuff and collapse of the La Garita caldera, triggered by magma chamber depressurization induced by eruption of the Pagosa Peak Dacite. More explosive eruptive style results from catastrophic magma escape along ring-fault vents.

of the Mt. St. Helens and Montserrat magmas were as much as 70–170°C higher. The low temperature of Fish Canyon magma (~760°C) may have retarded the kinetics of hornblende breakdown, but the appearance of microlites in the Pinatubo magma after short periods of degassing would appear to be an applicable constraint. Thus, if fracture-dominated fragmentation of the Fish Canyon magma during the Pagosa Peak eruption operated primarily due to low gas contents, degassing must have occurred shortly before fragmentation.

A major distinction between the Pagosa Peak Dacite and typical ignimbrite eruptions may be the rate of roof-rock subsidence. Slow foundering of fault blocks and the development of fissures, without catastrophic caldera collapse and accompanying sudden depressurization of the magma reservoir, may have permitted magma ascent rates higher than the 65–70 m/h needed to avoid hornblende breakdown (Rutherford and Hill, 1993), but slow enough to permit fissure-wall degassing due to the large surface area of such conduits. The large cross-sectional area of fissure vents would facilitate the high discharge rates needed to explain rapid emplacement of the deposit, without requiring the vent-emission velocities associated with plinian eruptions. The formation of many simultaneously active vents, thereby decreasing the initial emission velocity for a given discharge rate, has also been invoked for ignimbrite eruptions related to low-column pyroclastic fountaining (Branney and Kokelaar, 1992; Branney and Kokelaar, 1994).

5.3. Post-emplacement viscous flow

Two contrasting styles of viscous deformation apparently affected the Pagosa Peak deposits. Widespread rheomorphic flow flattened and stretched the pyroclastic fragments at high temperature, soon after emplacement. The horizontal fabric of most flow layering and the absence of complex folding in the deposits exclude large transport distances. This suggests that the driving force was gravitational spreading of the thickest accumulations, rather than wholesale mobilization leading to advancing flow fronts.

Distal sections southeast of Mount Hope deformed in a more brittle and kinematically complex style (Fig. 9). This deformation most likely accompanied the horizontal spreading of proximal sections, which pushed outward and ramped the less mobile distal rocks, deforming them by penetrative shear.

6. Conclusions

The Pagosa Peak Dacite is an atypical pyroclastic deposit. The observed characteristics are consistent with lateral transport as dense, poorly inflated pyroclastic flows, which accumulated locally to >1 km thick. Widespread rheomorphic flow of this viscous deposit, presumably due to gravitational spreading, required efficient heat retention and rapid emplacement. Although an origin as block-and-ash flows emplaced by collapse of enormous lava domes is possible, the deposit is more likely to have resulted from a low-column pyroclastic eruption (Fig. 12).

New field evidence and $^{40}Ar/^{39}Ar$ ages demonstrate that the Pagosa Peak Dacite is a less explosive precursor to eruption of the Fish Canyon Tuff (Fig. 12). Differences in eruptive mechanisms between these two units are probably unrelated to primary magmatic properties, as both were erupted in rapid succession from the same unzoned magma chamber. Varied rates of magma discharge versus degassing in the eruption conduit, influenced by different structures in the magma-chamber roof, may have been critical. The opening of multiple vents during fault-block subsidence may have allowed efficient degassing and low-column fountaining during the Pagosa Peak eruption. The absence of microlites or hornblende reaction rims constrains the timing of degassing to shortly before or during eruption. Depressurization of the enormous magma chamber during the proportionally smaller Pagosa Peak event may have led to instability of the magma chamber roof, thereby triggering eruption of the enormous Fish Canyon Tuff and formation of the La Garita caldera.

Acknowledgements

Many thanks to Christian Huber and Olivier Roche for strong-legged support during strenuous field seasons, to Jenni Barclay, Fidel Costa, Thao Ton-That, and Fleurice Parat for their advice, and to Jacques Metzger for his support on computer-aided drafting. We are grateful to participants of the 1997 informal San Juan workshop for helpful comments.

Reviews by Jake Lowenstern, Tim Druitt, and Wendell Duffield considerably improved the manuscript. Costs of fieldwork were supported by the USGS Volunteer Program, by Swiss FNRS grant # 20-49730.96, and by the Immanuel Friedlandes Foundation.

References

Best, M.G., Christiansen, E.H., 1997. Origin of broken crystals in ash-flow tuffs. Geol. Soc. Am. Bull. 109, 63–73.

Boudon, G., Camus, G., Gourgaud, A., Lajoie, J., 1993. The 1984 nuée ardente deposits of Merapi volcano, central Java, Indonesia: stratigraphy, textural characteristics, and transport mechanisms. Bull. Volcanol. 54, 327–342.

Branney, M.J., Kokelaar, P., 1992. A reappraisal of ignimbrite emplacement: progressive aggradation and changes from particulate to non-particulate flow during emplacement of high-grade ignimbrite. Bull. Volcanol. 54, 504–520.

Branney, M.J., Kokelaar, P., 1994. Volcanoteconic faulting, soft-state deformation, and rheomorphism of tuffs during development of a piece-meal caldera, English Lake District. Geol. Soc. Am. Bull. 106, 507–530.

Cashman, K.V., Mangan, M.T., 1994. Physical aspects of magma degassing II. Constraints on vesiculation processes from textural studies or eruptive products. Rev. Mineral. 30, 447–478.

Chapin, C.E., Lowell, G.R., 1979. Primary and secondary low structures in ash-flow tuffs of the Gribbles Run Paleovalley, central Colorado. Geol. Soc. Am. Spec. Pap. 180, 137–154.

Cole, P.D., Calder, E.S., Druitt, T.H., Hoblitt, R., Robertson, R., Sparks, R.S.J., 1998. Pyroclastic flows generated by gravitational instability of the 1996-7 lava dome of Soufrière Hills Volcano, Montserrat. Geophys. Res. Lett. 25 (18), 3425–3428.

Davis, J.M., Elston, W.E., Hawkesworth, C.J., 1993. Basic and intermediate volcanism of the Mogollon-Datil volcanic field: implications for mid-Tertiary tectonic transitions in southwestern New Mexico, USA. Geol. Soc. Spec. Publ. 76, 469–488.

Devine, J.D., Rutherford, M.J., Gardner, J.E., 1998. Petrologic determination of ascent rate for the 1995–1997 Soufrière Hills Volcano andesitic magma. Geophys. Res. Lett. 25 (19), 3673–3676.

Dingwell, D.B., Webb, S.L., 1989. Structural relaxation in silicate melts and non-Newtonian melt rheology in geologic processes. Phys. Chem. Minerals 16, 4351–4366.

Dingwell, D.B., Romano, C., Hess, K.-U., 1996. The effect of water on the viscosity of haplogranitic melt under P–T–X conditions relevant to silicic volcanism. Contrib. Mineral. Petrol. 124, 19–28.

Duffield, W.A., 1990. Eruptive fountains of silicic magmas and their possible effects on the Tin content of fountain-fed lavas, Taylor Creek Rhyolite, New Mexico. Geol. Soc. Am. Spec. Pap. 246, 251–262.

Eichelberger, J.C., Carrigan, C.R., Westrich, H.R., Price, R.H., 1986. Non-explosive silicic volcanism. Nature 323, 598–602.

Fink, J.H., Anderson, S.W., Manley, C.R., 1992. Textural constraints on effusive silicic volcanism: beyond the permeable foam model. J. Geophys. Res. 97 (B6), 9073–9083.

Gardner, J.E., Thomas, R.M.E., Jaupart, C., Tait, S., 1996. Fragmentation of magma during Plinian volcanic eruptions. Bull. Volcanol. 58, 144–162.

Geschwind, C.H., Rutherford, M.J., 1995. Crystallization of microlites during magma ascent: the fluid mechanics of the 1980–1986 eruptions at Mount St-Helens. Bull. Volcanol. 57, 356–370.

Hammer, J.E., Cashman, K.V., Hoblitt, R.P., Newman, S., 1999. Degassing and microlite crystallization during pre-climactic events of the 1991 eruption of Mt. Pinatubo, Phillipines. Bull. Volcanol. 60, 355–380.

Hess, K.U., Dingwell, D.B., 1996. Viscosities of hydrous leucogranite melts: a non-Arrhenian model. Am. Mineral. 81, 1297–1300.

Hildreth, W., Drake, R.E., 1992. Volcán Quizapu, Chilean Andes. Bull. Volcanol. 54, 93–125.

Hort, M., 1998. Abrupt change in magma liquidus temperature due to volatile loss or magma mixing: effects on nucleation, crystal growth, and thermal history of the magma. J. Petrol. 39, 1063–1076.

Houghton, B.F., Wilson, C.J.N., 1989. A vesicularity index for pyroclastic deposits. Bull. Volcanol. 51, 451–462.

Jaupart, C., Allègre, C., 1991. Gas content, eruption rate, and instabilities of eruption regime in silicic volcanoes. Earth Planet. Sci. Lett. 102, 413–429.

Johnson, M., Rutherford, M., 1989. Experimentally determined conditions in the Fish Canyon Tuff, Colorado, magma chamber. J. Petrol. 30, 711–737.

Klug, C., Cashman, K.V., 1996. Permeability development in vesiculating magmas: implications for fragmentation. Bull. Volcanol. 58, 87–100.

Larsen, E.S.J., Cross, W., 1956. Geology and petrology of the San Juan region, Southwestern Colorado. US Geol. Surv. Prof. Pap. 258, 303.

Lipman, P.W., 2000. The central San Juan caldera cluster: regional volcanic framework. In: Bethke, P.M., Hay, R.L. (Eds.), Ancient Lake Creede: its volcanotectonic setting, history and sedimentation and relation to mineralization in the Creede Mining District. Geol. Soc. Am. Spec. Publ. in press.

Lipman, P.W., Doe, B., Hedge, C., 1978. Petrologic evolution of the San Juan volcanic field, Southwestern Colorado: Pb and Sr isotope evidence. Geol. Soc. Am. Bull. 89, 59–82.

Lipman, P.W., Sawyer, D.A., Hon, K., 1996. Ash-flow sheets and calderas of the southeastern San Juan volcanic field, Colorado: new tales from old tuffs. Geol. Soc. Am. Bull. 108 (8), 1039–1055.

Lipman, P.W., Dungan, M.A., Brown, L., Deino, A., 1996. Ash-flow sheets and calderas of the southeastern San Juan volcanic field, Colorado: new tales from old tuffs. Geol. Soc. Am. Bull. 108 (8), 1039–1055.

Lipman, P.W., Dungan, M.A., Bachmann, O., 1997. Comagmatic granophyric granite in the Fish Canyon Tuff, Colorado: implications for magma-chamber processes during a large ash-flow eruption. Geology 25 (10), 915–918.

Mahood, G., 1984. Pyroclastic rocks and calderas associated with strongly peralkaline magmatism. J. Geophys. Res. 89, 8540–8553.

Mahood, G.A., Hildreth, W., 1986. Geology of the alkalic volcano at Pantellaria, Straits of Sicily. Bull. Volcanol. 48, 143–172.

Manley, C.R., 1996. In situ formation of welded tuff-like textures in the carapace of a voluminous silicic lava flow, Owyhee County, SW Idaho. Bull. Volcanol. 57, 672–686.

Milner, S.C., Duncan, A.R., Ewart, A., 1992. Quartz-latite rheoignimbrite flows of the Etendeka Formation, north-western Namibia. Bull. Volcanol. 54, 200–219.

Moore, I., Kokelaar, P., 1998. Tectonically-controlled piecemeal caldera collapse: a case study of Glencoe volcano, Scotland. Geol. Soc. Am. Bull. 110, 1448–1466.

Papale, P., 1999. Strain-induced magma fragmentation in explosive eruptions. Nature 397, 425–428.

Plouff, D., Pakiser, L.C., 1972. Gravity study in the San Juan Mountains, Colorado. US Geol. Surv. Prof. Pap. 800, B183–B190.

Renne, P.R., et al., 1998. Intercalibration of standards, absolute ages and uncertainties in $^{40}Ar/^{39}Ar$ dating. Chem. Geol. 145, 117–152.

Riciputi, L.R., Johnson, C.M., Sawyer, D.A., Lipman, P.W., 1995. Crustal and magmatic evolution in a large multicyclic caldera complex: isotopic evidence from the central San Juan volcanic field. J. Volcanol. Geotherm. Res. 67, 1–28.

Rodriguez-Elizarras, S., Siebe, C., Komorowski, J.C., Espindola, J.M., Saucedo, R., 1991. Field observations of pristine block-and-ash-flow deposits emplaced April 16–17, 1991 at Volcan de Colima, Mexico. J. Volcanol. Geotherm. Res. 48, 399–412.

Rutherford, M.J., Hill, P.M., 1993. Magma ascent rate from amphibole breakdown: an experimental study applied to the 1980–1986 Mount St-Helens eruptions. J. Geophys. Res. 98 (B11), 7–19685.

Scaillet, B., Holtz, F., Pichavant, M., 1998. Phase equilibrium constraints on the viscosity of silicic magmas 1. Volcanic–plutonic comparison. J. Geophys. Res. 103 (B11), 27 257–27 266.

Schmincke, H.U., Swanson, D.A., 1967. Laminar viscous flowage structures in ash-flow tuffs from Gran Canaria, Canary Islands. J. Geol. 75, 641–664.

de Silva, S.L., Self, S., Francis, P.W., Drake, R.E., Carlos Ramirez, R., 1994. Effusive silicic volcanism in the Central Andes: the Chao dacite and other lavas of the Altiplano–Puna Volcanic Complex. J. Geophys. Res. 99 (9), 17805–17825.

Smith, T.R., Cole, J.W., 1997. Somers Ignimbrite Formation: Cretaceous high-grade ignimbrites from South Island, New Zealand. J. Volcanol. Geotherm. Res. 75, 39–57.

Sparks, R.S.J., 1978. The dynamics of bubble formation and growth in magmas: a review and analysis. J. Volcanol. Geotherm. Res. 3, 1–37.

Sparks, R.S.J., 1997. Causes and consequences of pressurization in lava dome eruptions. Earth Planet Sci. Lett. 150, 177–189.

Stasiuk, M.V., et al., 1996. Degassing during magma ascent in the Mule Creek vent (USA). Bull. Volcanol. 58, 117–130.

Steven, T.A., 1975. Mid-Tertiary volcanic field in the southern Rocky Mountains. Geol. Soc. Am. Mem. 144, 75–94.

Swanson, S.E., Namey, M.T., Westrich, H.R., Eichelberger, J.C., 1989. Crystallization history of Obsidian Dome, Inyo Domes, California. Bull. Volcanol. 51, 161–176.

Thomas, N., Jaupart, C., Vergniolle, S., 1994. On the vesicularity of pumice. J. Geophys. Res. 99 (B8), 15633–15644.

Turbeville, B.N., 1992. Tephra fountaining, rheomorphism, and spatter flow during emplacement of the Pitigliano Tuffs, Latera caldera, Italy, . J. Volcanol. Geotherm. Res. 53, 309–327.

Twist, D., Elston, W.E., 1989. The Rooiberg felsite (Bushveld complex): textural evidence pertaining to emplacement mechanisms for high-temperature siliceous flows. New Mex. Bur. Mines Res. Bull. 131, 274.

Ui, T., Matsuwo, N., Sumita, M., Fujinawa, A., 1999. Generation of block and ash flows during the 1990–1995 eruption of Unzen Volcano, Japan. J. Volcanol. Geotherm. Res. 89, 123–137.

Walker, G.P.L., 1983. Ignimbrite types and ignimbrite problems. J. Volcanol. Geotherm. Res. 17, 65–88.

Whitney, J.A., Stormer, J.C., 1985. Mineralogy, petrology and magmatic conditions from the Fish Canyon Tuff, Colorado. J. Petrol. 26 (3), 726–762.

Wilson, C.J.N., Houghton, B.F., Kamp, P.J., McWilliams, M.O., 1995. An exceptionally widespread ignimbrite with implications for pyroclastic flow emplacement. Nature 378, 605–607.

Wilson, L., Sparks, R.S.J., Walker, G.P.L., 1980. Explosive volcanic eruptions—IV. The control of magma properties and conduit geometry on eruption column behavior. Geophys. J. Res. Astr. Soc. 63, 117–148.

Woods, A.W., Koyaguchi, T., 1994. Transitions between explosive and effusive eruptions of silicic magmas. Nature 370, 641–644.